SPIN-0 RBIT INTERACTION IN NEUTRON STAR/MAIN SEQUENCE BINARIES AND IMPLICATIONS FOR PULSAR TIMING

DONG LAI

Theoretical Astrophysics, 130-33, California Institute of Technology

Pasadena, CA 91125

1: dong@tapir.caltech.edu

LARS BILDSTEN

Department of Physics and Department of Astronomy

University of California, Berkeley, CA 94720

I: bildsten@fire.berkeley.edu

VICTORIA M. KASP11

David W. Morrisroe Astroscience Laboratory

11'AC/Caltech/Jet Prepulsion Laboratory, Pasadena, CA 91125

1: vicky@ipac.caltech.edu

ABSTRACT

The spin-induced quadruple moment of a rapidly rotating star changes the orbital dynamics in a binary system, giving rise to advance (or regression) of periastron and precession of the orbital plane. We show that these, effects are important in the recently discovered radio pulsar/main sequence star binary system PSR J0045−7319, and reliably account for the observed peculiar timing residuals. Precise measurements of the apsidal motion and orbital plane precession can yield valuable information on the internal structure and rotation of the star. The detection of orbital precession implies that the spin of the companion star is not aligned with the orbital angular momentum, and suggests that tile supernova gave the pulsar a kick out of the original orbital plane. Excitations of g-mode oscillations near periastron (the dynamical tide)

[1] Hubble Fellow; Visiting Associate, Caltech Astronomy Department.

can induce measurable changes in the orbital period and eccentricity at each passage for this system. We also discuss the spin-orbit coupling effects for the accreting X-ray pulsars and the other known radio pulsar/main sequence binary, PSR B 1259–63.

Subject headings: binaries: close - pulsars: individual: PSR J0045 --7319, PSR B 1259-63- stars: early type - stars: rotation stars: oscillations

1. INTRODUCTION

The discovery of radio pulsars in binary systems with massive main sequence stars (PSR B 1259—63, Johnston et al. 1992, 1994 and PSR J0045–7319, Kaspi et al. 1994) makes it possible to measure apsidal motion and other hydrodynamical effects on the pulsar orbit. Indeed, the detection of large (≈ 30 msec) *frequency-independent* timing residuals from PSR J0045–7319 (Kaspi et al. 1995a) has motivated our consideration of the dynamical effects caused by the spin- induced quadruple on the stellar companion. his is expected to be the dominant effect, as massive main sequence stars are fast rotators and typically have rotation periods on the order of days (Jaschek & Jaschek 1987). We show that the spin-orbit coupling in these systems is indeed significant, and leads to both apsidal motion and precession of the orbital plane that can account for the timing residuals seen in PSR J0045–7319.

The information learned from pulsar/main sequence binaries will complement the studies of double main sequence binaries, many of which have large enough quadrupoles (either from tides or fast rotation) to cause measurable apsidal motion in their eccentric orbits. As reviewed by Claret & Gimenez (1.993), the apsidal motion is combined with information on the stellar masses, radii and spins to yield the apsidal constant, k, which is a dimensionless measure of the density concentration Of the stellar interior. These measurements compare favorably With those expected from theoretical stellar structure models (see Claret & Gimenez 1993 for the few exceptions). The pulsar systems considered here are most sensitive to the spin-induced quadruple, permitting better studies of the orientation and magnitude of the spin of the stellar companion. Both of these quantities are important to constrain and/or measure in the context of mass transfer prior to the supernova and “kicks)' during the neutron star birth.

We start in §2 by explaining why the spin-induced quadrupole is important for these systems and then summarize the full equations for the precession and apsidal motion, correcting some previous typographical errors. We then show in §3 that the induced time delay is large and easily measurable for the two radio pulsars under consideration, PSR J0045–7319 and PSR B1259–63 We demonstrate that this effect is present in the timing data of PSR J0045- -7319. In particular, the unusual residuals observed by Kaspi et al. (1995a) are the result of fitting a purely Keplerian orbit to irregularly sampled data in which apsidal advance and orbital precession are present. Section 4 cent sins simple estimates of other effects that might prove important, including tidal effects and general relativity. We show that tidal excitations of high-order gravity modes in tile companion near periastron can yield pleasurable changes in the orbital period and eccentricity. We conclude in §5 by outlining the prospects for constraining the system parameters of PSR J0045– 7319, and the possibilities for similar measurements in accreting X-ray pulsars.

2. SPIN-ORBIT COUPLING IN BINARY SYSTEMS

The neutron star's gravitational field couples to both the tide-induced quadrupole and the spin-induced quadrupole of the stellar companion. We begin by comparing the relative magnitudes of these two effects. The tidal bulge on the stellar companion has a height $h \sim M_p R_c^4/(M_c r^3)$, where M_c and R_c are the companion mass and radius, M_p is the pulsar (neutron star) mass, and r is the instantaneous center of mass separation. The tidal quadrupole is then roughly

$$Q_{\rm tide} \sim k M_c R_c^2 \left(\frac{h}{R_c}\right) \sim k M_p R_c^2 \left(\frac{R_c}{r}\right)^3 . \tag{1}$$

We compare this to the quadrupole induced by rotation at angular velocity, $\Omega_s = 2\pi/P_s$,

$$Q_{\rm spin} \sim k M_c R_c^2 \frac{\Omega_s^2 R_c^3}{(GM_c)} . \tag{2}$$

At periastron, the ratio of these two is

$$\frac{Q_{\rm spin}}{Q_{\rm tide}} \sim \left(\frac{P_{\rm orb}}{P_s}\right)^2 \frac{(M_p + M_c)}{M_p} (1 - e)^3, \tag{3}$$

where $P_{\rm orb}$ and e are tile orbital period and eccentricity. Equation (3) shows that neutron stars which orbit massive stellar companions having rotation frequencies shorter than the orbital frequency are most sensitive to the spin-induced quadrupole. Binary systems containing early-type stars (in particular those with convective cores and radiative envelopes) with orbital periods longer than $2-3$ days are not expected to circularize and synchronize appreciably in a time comparable to the main sequence life span (Zahn 1977). Both PSR B1259$-$63 and PSR J0045$-$7319 are of this type and, as we describe in §3, are timed with sufficient accuracy for these effects to be measurable.

2.1 Spin-Induced Distortion

The quadruple from the rotational distortion of the finite-sized companion is specified by the difference between the moments of inertia about the spin axis, I_3, and an orthogonal axis, I_1. Claret & Gimenez (1992) calculated the moment of inertia for slowly rotating main sequence stars. We incorporate their results by introducing a parameter λ, whose value is close to unity, so that

$$I_3 = 0.1\lambda M_c R_c^2. \tag{4}$$

(The parameter λ also accounts for the increase of the equatorial radius of the rotating star, which can be as large as $3R_c/2$ near the maximum rotation rate). The quadruple from the rotational distortion of the star is proportional to the spin squared. Following the conventional definition of the apsidal motion constant k (Cowling 1938; Schwarzschild 1958), we write

$$I_3 - I_1 = \frac{2}{3} k M_c R_c^2 \hat{\Omega}_s^2, \tag{5}$$

where $\hat{\Omega}_s$ is the dimensionless spin $\hat{\Omega}_s \equiv \Omega_s/(GM_c/R_c^3)^{1/2}$ of the companion. For stars with uniform density, $k = 3/4$. For the $M_c \approx 10M_\odot$ main-sequence star of interest here, $k \simeq 0.01$, depending on the stellar age (Schwarzschild 1958; Claret & Gimenez 1992). Although strictly speaking expression (4) is valid only for $\hat{\Omega}_s \ll 1$, for convenience we will use it even when the spin rate is close to the brink-up value $\hat{\Omega}_{s,max} = 1.5^{-3/2} \simeq 0.5$

2.2 Spin-Induced Apsidal Motion and Orbital Precession

Because of the spin-induced quadrupole moment, the potential between the components deviates from $-GM_cM_p/r$ by an amount

$$\Delta V = -\frac{GM_p(I_3 - I_1)}{2r^3}\left(1 - 3\sin^2\theta\cos^2\psi\right), \tag{6}$$

where θ is the angle between the orbital angular momentum $\mathbf{L}$ and the spin angular momentum $\mathbf{S}$, and ψ is the orbital phase ($\psi = 0$ when the pulsar lies in the plane defined by $\mathbf{L}$ and $\mathbf{S}$). This leads to apsidal motion (advance or regression of the longitude of periastron) and, when the spin $\mathbf{S}$ is not aligned with the orbital angular momentum $\mathbf{L}$, a precession of the orbital plane. The general expressions for the rates of apsidal motion and orbital precession have been derived by Smarr & Blandford (1976) and Kopal (1978) using standard celestial mechanics perturbation theory. In the coordinates of Figure 1, the rate of change of the dynamical longitude of periastron (measured from the ascending node in the invariable plane perpendicular to $\mathbf{J} = \mathbf{L} + \mathbf{S}$), χ, is given by

$$\dot{\chi} = \frac{3\pi(I_3 - I_1)}{M_ca^2(1 - e^2)^2P_{\rm orb}}\left(1 - \frac{3}{2}\sin^2\theta + \frac{1}{2}\sin 2\theta\cot\theta_c\right), \tag{7}$$

where a is the semi-major axis of the (relative) orbit, and θ_c is the angle between $\mathbf{L}$ and $\mathbf{J}$.[2]

The orbital plane precession rate can also be obtained using perturbation theory. More directly, we can obtain it be considering the interaction torque between the stars. After averaging over one orbital period, the torque acting on the orbit is given by

$$\mathbf{N} = \frac{3GM_p(I_3 - I_1)\cos\theta\,\mathbf{S}\times\mathbf{L}}{2a^3(1 - e^2)^{3/2}SL}, \tag{8}$$

The precession rate $\mathbf{\Omega}_{\rm prec} = \dot{\Phi}\hat{\mathbf{J}}$ (cf. Fig. 1) of $\mathbf{L}$ around $\mathbf{J}$ is therefore

$$\mathbf{\Omega}_{\rm prec} = -\frac{3GM_p(I_3 - I_1)\cos\theta}{2a^3(1 - e^2)^{3/2}}\frac{\mathbf{J}}{SL} = -\frac{3\pi(I_3 - I_1)}{M_ca^2(1 - e^2)^2P_{\rm orb}}\left(\frac{\sin\theta\cos\theta}{\sin\theta_c}\right)\hat{\mathbf{J}}, \tag{9}$$

---

[2] This can be derived following the perturbation procedure of §11-3.C of Goldstein (1980), except that here the action variables are $J_1 = 2\pi L\cos\theta_c$, $J_2 = 2\pi L$, and note that the perturbation Hamiltonian (11-58) depends on θ (or i in Goldstein's notation), the angle between $\mathbf{L}$ and $\mathbf{S}$. Note that in Eq. (3.10) of Smarr & Blandford (1976), $\sin^2(\delta + \theta)$ should be $\sin 2(\delta + \theta)$; also in Eq. (11-60) of Goldstein (1980), the factor $(1 - e^2)^{-1}$ should be $(1 - e^2)^{-2}$.

where the minus sign implies that $\mathbf{L}$ precesses in a direction opposite to J, and we have used $L = [GM_p^2 M_c^2 a(1 - e^2)/M_t]^{1/2}$ for the Keplerian orbital angular momentum. In the limit of small mass ratio $M_p \ll M_c$ and $S \gg L$, where $S = |\mathbf{S}|$ and $L = |\mathbf{L}|$, equations (7) and (9) reduce to the rates of apsidal motion and orbital precession for the Earth-satellite system (Goldstein 1980). By contrast, for binary pulsars of interest in this paper, $L >> S$. Using the moment of inertia and quadrupole from equations (4) and (5) we obtain

$$\Omega_{\rm prec} \simeq -\Omega_{\rm orb} \frac{10kM_p}{\lambda(M_c M_t)^{1/2}} \left(\frac{R}{a}\right)^{3/2} \frac{\hat{\Omega}_s \cos\theta}{(1-e^2)^{3/2}}, \tag{10}$$

where $M_t = M_p + M_c$. The angle of the precession cone (i.e., the angle between $\mathbf{L}$ and J) is given by

$$\theta_c \simeq \frac{S\sin\theta}{L} \simeq \frac{\lambda(M_c M_t)^{1/2}}{10M_p} \left(\frac{R_c}{a}\right)^{1/2} \frac{\hat{\Omega}_s \sin\theta}{(1-e^2)^{1/2}}, \tag{11}$$

in the $L >> S$ limit.

It should be noted that the derivation of the above equations assumes the companion star behaves as a rigid body. One might be concerned that fluid stars respond to external forces differently than a rigid object (Smarr & Blandford 1976; Papaloizou & Pringle 1982), This is by no means a resolved issue, although it seems unlikely that deviation from rigid body behavior is large since the tidal distortion of the star is small compared to the rotational distortion. The observations of these pulsars may well provide information on this subtlety.

2.3 Effects on the Observables

The apsidal motion and orbital plane precession change w, the observational longitude of periastron (measured from the ascending node in the plane of the sky), and i, the orbital inclination angle (the angle between $\mathbf{L}$ and $\mathbf{n}$, the unit vector along the line-of-sight). Let i_o be the angle between $\mathbf{J}$ and $\mathbf{n}$ (see Fig. 1), in which case the observational angles ω and i are related to χ and Φ by:

$$\begin{aligned} \sin\omega &= \frac{1}{\sin i}[(\sin\theta_c\cos i_o + \cos\theta_c \sin i_o \cos\Phi)\sin\chi + \sin i_o \cos\chi \sin\Phi]\,, \\ \cos i &= -\sin\theta_c \sin i_o \cos\Phi + \cos i_o \cos\theta_c. \end{aligned} \tag{12}$$

For $L >> S$ or $\theta_c << 1$, these reduce to $\omega \simeq \chi + \Phi$ and $i \simeq i_o + \theta_c \cos \Phi$. Using equations (5), (7) and (9), we then have

$$\dot{\omega} \simeq \frac{3\pi(I_3 - I_1)}{M_c a^2 (1-e^2)^2 P_{\rm orb}} \left(1 - \frac{3}{2}\sin^2\theta\right) \simeq \Omega_{\rm orb} \frac{k R_c^2 \hat{\Omega}_s^2}{a^2(1-e^2)^2} \left(1 - \frac{3}{2}\sin^2\theta\right), \quad (13)$$

and

$$\frac{di}{dt} \simeq \frac{3\pi(I_3 - I_1)}{M_c a^2 (1-e^2)^2 P_{\rm orb}} \sin\theta\cos\theta\sin\Phi \simeq \Omega_{\rm orb} \frac{k R_c^2 \hat{\Omega}_s^2}{a^2(1-e^2)^2} \sin\theta\cos\theta\sin\Phi. \quad (14)$$

Thus for typical θ and Φ, the numerical value of di/dt is comparable to that of $\dot{\omega}$. Note that the observed apsidal motion is an advance for $\sin\theta < (2/3)^{1/2}$ and a regression in the opposite case. In addition, twice in one precession cycle, at $\Phi = 0$ and π (i.e., when **J**, **L** and **n** lie in the same plane), the rate di/dt for the change of the orbital inclination angle is identically zero.

3. SPIN-ORBIT EFFECTS ON BINARY PULSAR TIMING

We now consider the effects of spin-orbit coupling on the timing of the two binary pulsar systems with main-sequence-star companions. The orbital motion gives rise to a delay of $T(t) = \mathbf{r}_p \cdot \mathbf{n}/c = r_p(t) \sin\Psi(t) \sin i(t)/c$ in the pulse arrival time, where $\mathbf{r}_p = \mathbf{r} M_c/(M_p + M_c)$ is the pulsar position vector. The orbital phase (or true anomaly) $\Psi(t)$ measured from the observational ascending node is given by $\Psi(t) = \Psi(t)_K + \dot{\omega} t$, where $\Psi(t)_K$ is the Keplerian value. The longitude of periastron $\omega(t)$ and the orbital inclination angle $i(t)$ vary according to equations (13) and (14), with the precession phase given by $\Phi(t) = \Omega_{\rm prec} t + \Phi_0$.

We are interested in the residual $\delta T(t) \equiv \mathbf{r}_p \cdot \mathbf{n}/c - (\mathbf{r}_p \cdot \mathbf{n}/c)_K$ of the time delay compared to the Keplerian value. For $t << 1/|\Omega_{\rm prec}|$ and $t << 1/|\dot{\omega}|$, we have $\delta T = \delta T_{\rm aps} + \delta T_{\rm prec}$, where the contributions from apsidal motion and orbital plane precession are given by (assuming $\delta T = 0$ at $t = 0$)

$$\begin{aligned} \delta T(t)_{\rm aps} &\simeq \frac{r_p(t)}{c} \sin i_o \cos\Psi(t)\, \dot{\omega}\, t, \\ \delta T(t)_{\rm prec} &\simeq \frac{r_p(t)}{c} \cos i_o \sin\Psi(t)\, \frac{di}{dt}\, t. \end{aligned} \quad (15)$$

Clearly, the residual resulting from the neglect of varying w and i in the timing model increases with t, and is modulated by tile orbital motion 3 Equations (15) are the leading order corrections for this effect, and are valid for time scales much less than the precession period, which is $\sim$ 300 yearsfor PSR J0045–7319 (see §3.1). The next order terms are of order $\dot{\omega}t$ or $(di/dt)t$ smaller and have different dependences on i and Ψ. The accumulation of accurate timing data over a longer baseline will further constrain the system.

3.1 PSR J0045–7319

Radio timing observations by Kaspi et al. 1994 of the 0.93 s pulsar PSR J0045–7319 have identified it to be in an eccentric ($e = 0.8080$) 51.17 day orbit having projected semi-major axis $a_p \sin i/c = 174$ s. They made optical observations in the direction of the pulsar and found a B1V star with $B = 16.03$ and $V = 16.19$ which showed no evidence for emission lines. Combining the effective temperature ($T_{\rm eff} \approx 2.4 \times 10^4$ K) and reddening ($A_V \simeq 0.27$) with the observed colors gives $R_c \simeq (6.4 + 0.5) R_\odot (d/59\,{\rm kpc})$. The optical radial velocity measurements of the B star fix its mass to be $(8.8 \pm 1.8) M_\odot$ for $M_p = 1.4 M_\odot$ and give $i = 44 \pm 5$ degrees (Bell et al. 1995). This then yields $a \simeq 126 R_\odot \simeq 20 R_c$. The rotational velocity $v_{rot} \sin\theta_{sn} \simeq 195 \pm 20$ km/s (where θ_{sn} is the angle between S and n) obtained from spectral line broadening (Bell et al.1995) is consistent with rapid rotation near break-up, $\hat{\Omega}_s \sim 0.5$, confirming that the system is not synchronized. Equations (10), (13) and (14) then give

$$
\begin{aligned}
\Omega_{\rm prec} &\simeq -1.9 \times 10^{-2} \lambda^{-1} \left(\frac{k}{0.01}\right)\left(\frac{20R_c}{a}\right)^{3/2}\left(\frac{\hat{\Omega}_s}{0.5}\right) \cos\theta \ \frac{\rm rad}{\rm yr}, \\
\dot{\omega} &\simeq 2.3 \times 10^{-3} \left(\frac{k}{0.01}\right)\left(\frac{20R_c}{a}\right)^{2}\left(\frac{\hat{\Omega}_s}{0.5}\right)^2 \left(1 - \frac{3}{2}\sin^2\theta\right) \frac{\rm rad}{\rm yr}, \qquad (16) \\
\frac{di}{dt} &\simeq 2.3 \times 10^{-3} \left(\frac{k}{0.01}\right)\left(\frac{20R_c}{a}\right)^{2}\left(\frac{\hat{\Omega}_s}{0.5}\right)^2 \sin\theta\cos\theta\sin\Phi \ \frac{\rm rad}{\rm yr}.
\end{aligned}
$$

[3]Note that for very eccentric systems, the changes in w and i mainly occur near periastron, rather than accumulating uniformly throughout the orbital period. We neglect this finer point in equation (15).

The timing residual AT accumulated in one orbit is estimated by setting $r_p \simeq 2a_p$ and $t \simeq P_{\rm orb}/2$ in equation (lb), giving

$$\Delta T_{\rm aps} \simeq \frac{a_p \sin i}{c} \dot{\omega} P_{\rm orb} \simeq 56 \left(\frac{k}{0.01}\right)\left(\frac{20R_c}{a}\right)^2\left(\frac{\hat{\Omega}_s}{0.5}\right)^2\left(1 - \frac{3}{2}\sin^2\theta\right) \text{ ms},$$

$$\Delta T_{\rm prec} \simeq \frac{a_p \cos i}{c}\frac{di}{dt} P_{\rm orb} \simeq 56 \left(\frac{k}{0.01}\right)\left(\frac{20R_c}{a}\right)^2\left(\frac{\hat{\Omega}_s}{0.5}\right)^2\left(\frac{\cos i}{\sin i}\sin\theta\cos\theta\sin\Phi\right) \text{ ms}. \tag{17}$$

The modulated residual in just one orbit is thus comparable to the residuals found by Kaspi et al. (1995a.).

3.2 PSR 111259-63

This 47.76 ms pulsar is in an eccentric orbit with an Be star companion with $P_{\rm orb} = 1236$ days, c $= 0.8698$, and a_p *sin* $i/c = 1296$ s (Johnston et al. 1992, 1994). The optical data for this emission line star are still inadequate to place strong constraints on the spectral type and hence radius of the star, so we will use the fiducial values chosen by Johnston et al. (1994), $R_c = 6R_\odot$ and $M_c =$ 10 MO. For $M_p = 1.4M_\odot$, wc obtain a $= 1091R_\odot = 182R_c$. For typical values ($\lambda \simeq 1$, $k \simeq 0.01$ and $\hat{\Omega}_s \sim 0.5$) we get $\Omega_{\rm prec} \sim -4.1 \times 10^{-5}\cos\theta$ rad/yr, $\dot{\omega} \simeq 2.4 \times 10^{-6}(1 - 3/2 \sin^2\theta)$ rad/yr, and $di/dt \simeq 2.4 \times 10^{-6} \sin\theta\cos\theta\sin\Phi$ rad/yr. The timing residual accumulated in one orbit is given by

$$\begin{aligned}\Delta T_{\rm aps} &\simeq 10 \left(\frac{k}{0.01}\right)\left(\frac{182R_c}{a}\right)^2\left(\frac{\hat{\Omega}_s}{0.5}\right)^2\left(1 - \frac{3}{2}\sin^2\theta\right) \text{ ms},\\ \Delta T_{\rm prec} &\simeq 10 \left(\frac{k}{0.01}\right)\left(\frac{182R_c}{a}\right)^2\left(\frac{\hat{\Omega}_s}{0.5}\right)^2\left(\frac{\cos i}{\sin i}\sin\theta\cos\theta\sin\Phi\right) \text{ ms}.\end{aligned} \tag{18}$$

Thus AT can potentially affect the timing parameters for this system as well. Indeed, using a pure Keplerian model for the system resulted in substantial systematic timing residuals (Johnston et al. 1994; Manchester et al. 1995). ¿ From our estimate above, it is clear that these residuals may well have a significant contribution from the unfitted $\dot{\omega}$ and di/dt. A full understanding of this system will be complicated by the dispersion and radio eclipse caused by the wind from the Be star.

Note that the expressions given in §2 describe the *secular* change of the orbit, i.e., they are obtained by orbital averaging. To model closely -sampled timing data spanning only a few orbits, as in PSR, 111259-63, a numerical integration of the orbit with the perturbing potential given by equation (6) is required.

3.3 Data Fitting and the Observed Residual in PSR J0045−7319

Using multi-frequency radio timing observations of PSR J0045−7319, Kaspi et al. (1995a) showed that the observed barycentric pulse arrival times deviated significantly from those expected from a pure Keplerian orbit. In particular, they found significant *frequency-independent timing* residuals for a ∼10 day duration around periastron. These residuals showed systematic variations on time scales of a few days after subtraction of a Keplerian orbital fit to the entire 3.3 year data span. The residuals from two periastron observations separated by 11 orbits showed very different trends, inconsistent, with a simple! error in any of the Keplerian parameters. They noted that such residuals were unlike those of any other pulsar, isolated or binary.

We show here that the unusual PSR J 0045--7319 residuals can be explained by the relatively long-term dynamical effects described above, in spite of the former's apparent short-time-scale variations. To do this, we simulated timing observation for a binary pulsar which has Keplerian parameters similar to those of PSR J0045−7319, but in addition has two post-Keplerian parameters, the apsidal advance $\dot{\omega}$ and a time-variable projected semi-major axis $\dot{x}$, where $x = a_p \sin i$. In the simulation, x and ω were. incremented by 0.0044 It-s and 0.0035° per orbit at periastron, which gave the Lest match to the observed residuals, These numbers correspond to $\dot{\omega} \sim$ 4,4 x 10^{-4} rad/yr and $di/dt \sim$ 1,8 x 10^{-4} rad/yr, consistent with equation (16). The actual fit to 'the data from PSR J0045−7319 and the implications for that source in particular will be discussed elsewhere (Kaspi et al. 1995b).

Tile simulated data were then fitted with a pure Keplerian orbit, holding all post-Keplerian parameters fixed at zero, thus simulating the analysis done by Kaspi et al. (1995a). The residuals for this fit are shown in the upper panel of Figure 2. The effect of the post-Keplerian parameters is obvious as an orbital period modulation of increasing amplitude relative to the fitting epoch (cf. eq. (15)). The fitted Keplerian parameters are biased *away* from the assumed values because of the least-squares fitting procedure; indeed the fitted solution shown in the Figure has '(spikes') for this reason. Next, using the same set of simulated arrival times, we selected those that coincide with actual observations of PSR J0045- 7319 at the Parkes observatory, in order to simulate the sampling interval used by Kaspi et al. (1995a) in their timing analysis. Again wc fit a simple Keplerian orbit, holding all post-I{ eplerian parameters fixed at zero. The resulting post-fit residuals are shown in the middle panel of Figure 2. Close-up views of the two epochs of periastron investigated by Kaspi et al. are shown in the bottom panels; a comparison with the data indicates that this model closely mimics the observed trends. Thus, we nave shown that the unusual residuals for PSR J0045−7319 can be explained as being a result of fitting a purely Keplerian orbit to infrequently and irregularly sampled data in which post-Keplerian apsi dal advance and orbital plane precession are significant.

4. OTHER EFFECTS

For completeness, we now discuss several effects that might change the binary orbit and compare them to the spin-orbit coupling effects discussed in §2-3.

4.1 Apsidal Motion due to Static Tide

Here we consider the standard tide-induced apsidal motion widely studied in stellar binaries (Cowling 1938; Schwarzschild 1958). It is assumed that at a given binary separation the star relaxes instantaneously to the equilibrium state. The resulting static. interaction potential is $V(r) = -GM_p M_c/r - kGM_p^2 R_c^5/r^6$. Assuming the orbital energy E and angular momentum L are constants, one obtains the standard formula (Cowling 1938)

$$\dot{\omega}_{\rm tide} = 15\,k\,\Omega_{\rm orb}\frac{M_p}{M_c}\left(\frac{R_c}{a}\right)^5\left(1+\frac{3}{2}e^2+\frac{1}{8}e^4\right)(1-e^2)^{-5}. \qquad (19)$$

For PSR J0045−7319, this gives $\dot{\omega}_{\rm tide} \sim 1.3 \times 10^{-4}(k/0.01)(20R_c/a)^5$ rad/yr, about an order of magnitude smaller than the spin-induced $\dot{\omega}$. This secular trend is degenerate with the spin-in duced quadrupole effect. For PSR B1259−63, $\dot{\omega}_{\rm tide} \simeq$

$2.7 \times 10^{-10}(k/0.01)(182\, R_c/a)^5$ rad/yr, four orders of magnitude smaller than the spin effects, and is completely negligible. Note that, unlike the spin induced quadruple, tidal effects cannot produce changes in the orbital inclination angle.

4.2 Excitations of Oscillation Modes: Dynamical Tide

Energy and angular momentum are transferred between the star and the orbit during each periastron passage, changing the orbital constants of motion, E and L. This occurs when the changing tidal potential near periastron excites stellar oscillations in the companion. The energy transfer ΔE during each periastron passage is estimated with the formalism of Press & Teukolsky (1977), who considered tidal excitations for a parabolic orbit.[4] In the quadruple order, this is given by

$$\Delta E \sim \frac{GM_p^2}{R_c}\left(\frac{R_c}{r_{min}}\right)^6 T_2(\eta), \tag{20}$$

where r_{min} is the binary separation at periastron, $\eta = (M_c/M_t)^{1/2}(r_{min}/R_c)^{3/2}$ is the ratio of the time for periastron passage and the stellar dynamical time, and the dimensionless function $T_2(\eta)$ (defined in Press & Teukolsky 1976) involves $l = 2$ nonradial stellar oscillation modes and the orbital trajectory. The resulting fractional change of the orbital size is simply $\Delta a/a = -\Delta E/E$, and the orbital period change is given by

$$\frac{|\Delta P_{\rm orb}|}{P_{\rm orb}} = \frac{3|\Delta a|}{2a} \sim 3\frac{M_p}{M_c}\left(\frac{R_c}{a}\right)^5 (1-e)^{-6} T_2(\eta). \tag{21}$$

The angular momentum transferred during periastron, $\Delta L \sim \Delta E (GM_c/R_c^3)^{-1/2}$ (Lai 1994) gives

$$\left|\frac{\Delta L}{L}\right| \sim \left|\frac{\Delta E}{E}\right| \left(\frac{M_t}{M_c}\right)^{1/2}\left(\frac{R_c}{a}\right)^{3/2} \frac{1}{2(1-e^2)^{1/2}}, \tag{22}$$

which is typically negligible compared to $|\Delta E/E|$. The resulting change in orbital eccentricity is then $\Delta e \sim (\Delta a/a)(1-e^2)/(2e)$.

[4] This formalism is also reasonably accurate for highly elliptic orbits. This is because most of the energy transfer takes place near periastron, where the kinetic energy and potential energy $\sim GM_pM_c/r_{min}$ are much larger than the binding energy $GM_pM_c/(2a)$, and the orbit resembles a parabolic trajectory.

To estimate the importance of the dynamical tidal effects, we compare Au/u with the fractional change (due to the static tide) of w in one orbit $\Delta\omega/(2\pi) = \dot{\omega}_{\rm tide} P_{\rm orb}/(2\pi)$:

$$\frac{|\Delta a/a|}{\Delta\omega/2\pi} \sim \frac{2T_2(\eta)}{15k} \frac{(1+e)^5}{(1-e)} \left(1 + \frac{3}{2}e^2 + \frac{1}{8}e^4\right)^{-1} . \tag{23}$$

For PSR J0045–7319, using the parameters of §3.1, we have $\eta \simeq 7.0$, and $T_2(\eta) \simeq 3.5 \times 10^{-4}$ for an $n = 3$ polytrope with adiabatic index $\Gamma_1 = 5/3$ (e.g., Lee & Ostriker 1986), where most contributions to $T_2(\eta)$ come from g-modes of radial order 5 – 9. This gives $|\Delta a/a| \sim 0.1\Delta\omega/(2\pi)$, implying that the perturbation due to energy transfer is much smaller than the tide-induced apsidal motion, and is therefore even smaller than the spin effects discussed in §2-3. This estimate agrees with the more detailed study by Kumar, Ao & Quataert (1995), who concluded that the correction to equation (19) from the dynamical tide is only $\sim 1\%$. The orbital period change due to the energy transfer is given by $|\Delta P_{\rm orb}|/P_{\rm orb} \sim 10^{-6}$, and the eccentricity change is $|\Delta e| \sim 10^{-7}$. For PSR 111269--63, again using the parameters of §3.2, we have $\eta \simeq 108$, for which $T_2(\eta)$ is extremely small, and the dynamical tidal effects are therefore completely negligible[5].

It is important to note that the actual values and signs of $\Delta P_{\rm orb}$ and Δe depend on the damping of the tidally excited g-modes. If the damping time is much longer than the orbital period, the energy transfer for an elliptical orbit will depend on the phases of the oscillations of different modes, and varies (both in magnitude and sign) from one passage to another. In this case, equation (21) only represents the typical magnitude of $\Delta P_{\rm orb}$, not a steady $\dot{P}_{\rm orb}$. On the other hand, if the damping time is much shorter than the orbital period, the energy transfer near periastron is a one-way process, i.e., only from the orbit to the star. Therefore $\Delta P_{\rm orb}/P_{\rm orb}$ and Δe are both negative, i.e., the orbit decays and circularizes.

[5] Kochanek (1993) has previously discussed the dynamical tidal effects in the context of **PSR** B 1259—63. However, the observational data available then did not allow him to draw any firm conclusion.

Radiative damping is the dissipation mechanism for g-modes in an early-type main sequence star. Depending on detailed stellar models, the typical damping time is of order 100 years, although some g-modes can be damped in less than a year (e.g., Unno et al. 1979). If such a short damping timescale applies to the high order g-modes excited in PSR J0045−7319, orbital decay and circularization may be observable in the timing data. A more accurate talc.ulat ion of this effect is complicated by the rapid rotation of the B-star, which changes the g-mode structure when the rotation frequency is comparable to the g-mode frequen ties.

4.3 General Relativistic Orbital Precessions

General relativity (GR) also introduces periastron advance and orbital plane precession (Landau & Lifshitz 1962; Barker & O'Connell 1975):

$$\dot{\chi}_{\rm gr} = \Omega_{\rm orb}\frac{3GM_t}{a(1-e^2)c^2}, \qquad \Omega_{\rm prec,gr} = \Omega_{\rm orb}\frac{3GM_p(1+M_c/3M_t)}{2a(1-e^2)c^2}. \tag{24}$$

The latter results from the geodetic precession of the companion star's spin (note that the spin angular momentum of the pulsar is much smaller than that of the! companion). For PSR J0045- -7319, using the paramet ers given in $3.1, we have $\dot{\chi}_{\rm gr} \simeq 6.7 \times 10^{-5}$ rad/yr, and $\Omega_{\rm prec,gr} \simeq 5.9 \times 10^{-6}$ rad/yr. Thus GR-induced periastron advance is comparable to the tidal effect, but one order of magnitude smaller than the Newtonian spin effect. The GR-induced orbital precession is three orders of magnitude smaller than the Newtonian spin-induced quadruple effect. For PSR B 12 59−63, the GR. effects are even smaller because of the larger orbit.

5. DISCI)SS1ON

Smarr & Blandford (1976) first discussed the Newtonian spin-orbit effects in the context of PSR B 1913+16, That companion turned out to be a neutron star, which renders t hese Newtonian effects completely negligible and facilitat es excellent t ests of general relativity (e.g., Taylor& Weisberg 1989). The recent discovery of two radio pulsar/main sequence star binaries, PSR **.10045 -7319** and PSR 111259--63, finally allows for measurements of tile apsidal motion and other hydrodynamical effects in binary pulsar systems. In this paper we have shown that the Newtonian spin-orbit coupling is particularly important in PSR J0045−7319 and PSR B 1259—63 systems.

5.1 Constraints on the Binary Systems and Evolution

When the spin-induced quadrupole is the dominant effect, measuring $\dot{\omega}$ and di/dt provides valuable information on the system: (i) the sign of $\dot{\omega}$ constrains the spin-orbit angle θ (cf. eq. (13)); (ii) the ratio of $\dot{\omega}$ and di/dt yields a relation between θ and Φ; (iii) the angle θ_{sn} is a function of t?, Φ and i. Knowing i and by choosing a reasonable range of θ_{sn} (e. g., for the PSR J0045−7319 system: since v_{rot} must be smaller than the break-up limit $\simeq$ 420 km/s, we have $|\sin\theta_{sn}| \lesssim$ 195/420 = 0.46), we obtain another relation between θ and Φ; (iv) With the angles determined from (i)-(iii), the observed values of $\dot{\omega}$ and di/dt then constrain the stellar structure and rotation rate of the companion. In addition, long-term timing observations will measure various angles in addition to $\dot{\omega}$ and di/dt, yielding additional constraints on the system parameters (see discussion following eq. (15)).

Other effects may prove important for these systems, including the apsidal motion due to tides and general relativity. The dynamical tide (§4.2) induces measurable changes in $P_{\rm orb}$ and e, However, a detailed theoretical treatment of this effect is complicated by the rapid rotation of the companion star.

The information obtained from the systems can have important implications for the evolution of neutron star binaries. For example, if mass transfer in the pre-supernova binary forces S to be parallel to L (a very likely scenario), then a non-zero spin-orbit angle in the pulsar/main-sequence star system implies that the supernova gave the neutron star a kick velocity out of the original orbital plane. From the values of θ and e of the current system (assuming that circularization and spin-orbit alignment are not efficient in the current system), one may actually constrain the kick velocity. Cordes & Wasserman (1984.) discussed how such kicks might misalign the *neutron star* spin from the orbital angular momentum in PSR 1913+ 16, giving rise to measurable geodetic precession.

5.2 X-ray Binaries

Insight into orbital plane precession might prove important for accreting X-ray pulsars as well. Apsidal motion has been searched for in eccentric accreting systems. In particular, the 2σ upper limit on the apsidal motion in the eccentric 8.9 day binary Vela X-1 (which contains a supergiant) is $\dot{\omega} = 1.6$ deg/yr (Deeter et al. 1987). Tamura et al. (1992) claimed a detection of apsidal motion in the eccentric Be system 4U 0115+63 at the level $\dot{\omega} = 0.030 \pm 0.016$ deg/yr. More recent observations of this source with the BATSE instrument (Cominsky, Roberts & Finger 1994) contradict the claim of Tamura et al. (1992), find no evidence for apsidal motion. However, these measurements could be biased by the fact that $a_x \sin i$ was assumed constant.

The less accurate arrival times makes the search for orbital plane precession in the accreting X-ray pulsars more difficult than for radio pulsars. However, the orbital parameters are sufficiently accurate that one can search for orbital precession through temporally separated measurements of $a_x \sin i$, the projected size of the orbit for the x-ray pulsar. The system 4U 0115+63, which orbits a Be-type star with $P_{\rm orb} = 24$ days and has $e = 0.34$ may experience $\Delta i \simeq 6 \times 10^{-3}$ rad over a 17 year baseline (from equation (14) assuming a $10\,M_\odot$ main sequence star with radius $R = 6R_\odot$, $k = 0.01$ and rotating slowly enough, $\hat{\Omega}_s \simeq 0.05$, or accidentally having $\sin^2\theta$ close to 2/3 so as not to violate the upper limit on $\dot{\omega}$ from Cominsky et al. 1994). This is a factor of 6 larger than the fractional error on $a_x \sin i$ measured in 1978 (Rappaport et al. 1978) and may well allow for a very sensitive measurement of the rotation of the Be star in this system.

We thank Roger Blandford for clarifying discussion. This work has been supported in part by NASA Grants NAGW-2394 to Caltech and NAG5-2819 to U.C. Berkeley. L.B. was supported as a Compton Fellow at Caltech through NASA grant NAG5-2666 during part of this work. V.M.K. thanks Dave Van Buren for useful discussions, is supported by a Hubble Fellowship through grant number HF-1061.01-94A from the Space Telescope Science Institute, which is operated by the Association of Universities for Research in Astronomy, Inc., under NASA contract NAS5-26555, and carried out research at the Jet Propulsion Laboratory, California Institute of Technology.

REFERENCES

Barker, B. M., & O'Connell, R. F. 1975, ApJ, 199, L25

Bell, J. F., Bessell, M. S., Stappers, B. W., Bailes, M. & Kaspi, V. 1995, ApJL, in press

Claret, A., & Gimenez, A. 1992, A&A Suppl., 96, 255

——————.1993, A&A, 277, 487

Cominsky, L., Roberts, M. & Finger, M. H. 1994 in *The* Second *Compton Symposium*, ed. C. E. Fichtel, N. Gehrels, & J. P. Norris (AIP: New York) p. 294

Cordes, J. M. & Wasserman, J. 1984, ApJ , 279, 798

Cowling, T. G. 1938, MNRAS, 98, 734

Deeter, J . E., Boynton, P. E., Lamb, F. K., & Zylstra, G. 1987, ApJ, 314, 634

Goldstein, H. 1980, Classical Mechanics, 2nd Ed. (Addison-Wesley), p. 512

Jaschek, C., & Jaschek, M. 1987, The Classification of Stars (Cambridge Univ. Press: New York)

Johnston, S. et al. 1992, ApJ, 387, L37

Johnston, S. et al. 1994, MNRAS, 268, 430

Kochanek, C. S. 1993, ApJ, 406, 638

Kopal, Z. 1978, Dynamics of Close Binary Systems (1). Reidel Pub.: Dordreicht, Holland), p 232

Kaspi, V. M., et, al. 1994, ApJ, 423, L43

Kaspi, V, M., Manchester, R, N., Bailes, M. & Bell, J. F. 1995a, Compact Stars in Binaries, IAU Symp. 165, ed. J. van Paradijs, E. P. J. van den Heuvel, & E. Kuulkers (Kluwer Dordrecht), in press.

Kaspi, V. M., et al. 1995b, in preparation.

Kumar, P., Ao, C. O., & Quataert, E. J. 1995, ApJ, in press

Lai, D. 1994, Ph.D. thesis, Cornell University

Landau, L. D., & Lifshitz, E. M. 1962, Classical Theory of Fields (Oxford: Pcrga-111011)

Lee, H. M., & Ostriker, J. P. 1986, ApJ, 310, 176

Manchester, R. N., et al. 1995, ApJL, in press

Papaloizou, J. C. B., & Pringle, J. E. 1982, MNRAS, 200, 49

Press, W. H., & Teukolsky, S. A. 1977, ApJ, 213, 183

Rappaport, S., Clark, G. W., Cominsky, L., Joss, P. C. & Li, F. 1978, ApJ, 224, L1

Schwarzsc:hf'1 ,1 M. 1958, Structure and Evolution of the Stars (1 'rinceton University Press)

Smarr, L. I,., & Blandford, R. D. 1976, ApJ, 207, 574

Tamura, K., Tsunemi, H., Kitamoto, S., Hayashida, I{. & Nagase, F. 1992, ApJ, 389, 676

Taylor, J. 11. & Weisberg, J. M. 1989, ApJ, 345, 434

Unno, W., Osaki, Y., Ando, II., & Shibahashi, 1 I. 1979, Nonradial oscillations of Stars (Univ. of Tokyo Press), pp. 205-217.

Zahn, J.-P, 1977, A&A, 57, 383

Figure Captions

FIG. 1.- Binary geometry and the definitions of different angles. The invariable plane (XY) is perpendicular to the total angular momentum vector $\mathbf{J} = \mathbf{L} + \mathbf{S}$, and the line-of-sight unit vector $\mathbf{n}$ lies in the YZ plane, making an angle i_o with J. The inclination of the orbit with respect to the invariable plane is θ_c (which is also the precession cone angle of L around J), while the orbital inclination with respect to the plane of the sky is i. The angle between L and S is θ. The orbital plane intersects the invariable plane at ascending node A, with a longitude Φ measured in the invariable plane (Φ is also the phase of the orbital plane precession), The dynamical longitude of periastron (point P), measured in the orbital plane, is χ. The observational longitude of periastron is w (not shown in the Figure).

FIG. 2.- Simulated pulse arrival times for PSR J0045- 7319. The upper panel shows the residuals from a fit of a pure Keplerian orbit to fake pulse arrival time data ("measured" daily for four years) for a binary pulsar like PSR tJO045–7319 in which apsidal advance and orbital plane precession are important. The middle panel shows the residuals from a fit of this fake data sampled only at those epochs coinciding with actual observations of the pulsar. The two vertical solid lines show epochs of periastron separated by 11 orbits. The lower panels show c.1osc-u]>s of those epochs; the! observed trends in the residuals are similar to those observed by Kaspi et al. (1995a).

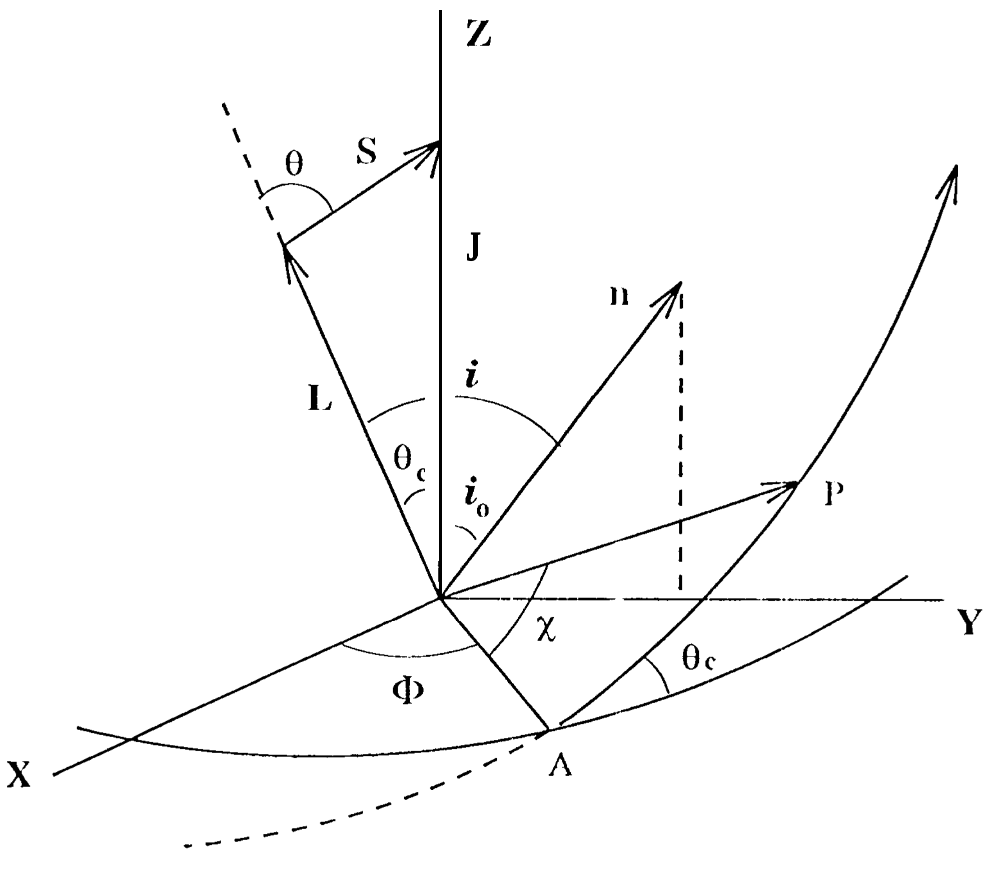
Z
S
θ
J
n
L
i
θc
io
P
Y
χ
θc
Φ
X
A

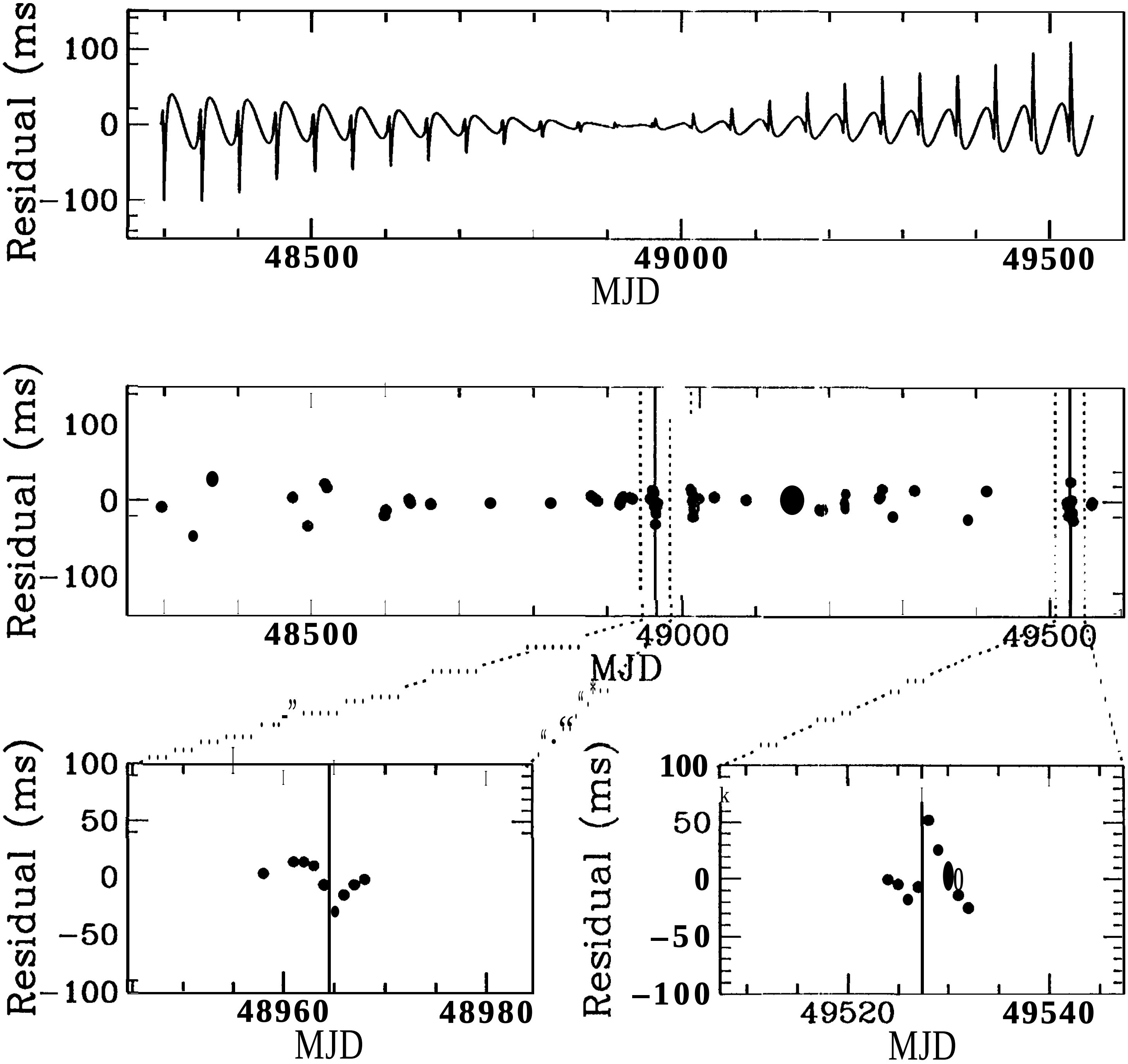

Residual (ms)
100
0
−100
48500
49000
49500
MJD
Residual (ms)
100
0
−100
48500
49000
49500
MJD
Residual (ms)
100
50
0
−50
−100
48960
48980
MJD
Residual (ms)
100
50
0
−50
−100
49520
49540
MJD

Fig. 2